

**INDUCED SPECTRAL BROADENING OF A WEAK  
PICOSECOND PULSE IN GLASS PRODUCED BY AN INTENSE  
PICOSECOND PULSE**

OPTICS LETTERS, 11, 626, 1986



# Induced spectral broadening of a weak picosecond pulse in glass produced by an intense picosecond pulse

R. R. Alfano, Q. X. Li, T. Jimbo, J. T. Manassah, and P. P. Ho

Department of Electrical Engineering, The City College of New York, New York, New York, 10031

Received February 7, 1986; accepted June 24, 1986

Spectral broadening of a weak 80- $\mu\text{J}$  picosecond 530-nm laser pulse in a BK-7 glass has been enhanced over the entire spectral band by the presence of an intense millijoule picosecond 1060-nm laser pulse. The spectral distributions of the self-phase modulation and the induced-phase modulation signals are similar. The dominant enhancement mechanism for the induced supercontinuum was determined to be caused by an induced-phase modulation process, not by stimulated four-photon scattering.

For many scientific and technological applications, it is important to have the capability to generate, transfer, and control a wide spectral bandwidth of ultrafast laser pulses. Sixteen years ago, Alfano and Shapiro<sup>1</sup> demonstrated that an ultrafast supercontinuum pulse (USP) covering a 10 000- $\text{cm}^{-1}$  frequency band with picosecond duration can be generated by propagating an intense picosecond laser pulse through condensed media. Since then, the USP has been applied to time-resolved absorption spectroscopy,<sup>2</sup> nonlinear optical effects,<sup>3</sup> and pulse compression.<sup>4</sup> The USP could also play an important role in applications in ranging, imaging, remote sensing, communication, and other fields.<sup>5,6</sup>

When an intense pulse propagates through a medium, it causes a refractive-index change. This in turn induces a phase change. The time variation of this phase will in turn cause a frequency sweep within the pulse envelope. This process is usually called self-phase modulation (SPM). When a weak probe pulse is sent into this disrupted system, the phase of the probe pulse at different frequencies can be modulated by the time variation of the nonlinear index of refraction originating from the primary intense pulse. This process is defined to be induced-phase modulation (IPM).<sup>7</sup> Both SPM and IPM give rise to spectral broadening for an ultrashort laser pulse.

In this Letter, we report the first observation to our knowledge of a weak second-harmonic centered induced ultrafast supercontinuum pulse (IUSP) generation due to the presence of a primary intense pulse in a BK-7 glass. The primary pulse at  $\omega_1$  induced the refractive change, causing a phase change and a frequency sweep of a probe pulse at  $2\omega_1$ . The enhancement of the bandwidth of the weak pulse at  $\lambda_2$  by propagating an intense laser pulse at  $\lambda_1$  in condensed media is attributed to IPM. This new effect has technological importance in communications and signal processing by permitting pulse coding in different frequency regions.

A single 8-psec laser pulse at 1060 nm generated from a mode-locked glass laser system was used as the pump beam. Its second harmonic (SH) was used as

the probe beam. These pulses at the primary 1060-nm and the SH 530-nm wavelengths were weakly focused into a 9-cm-long BK-7 glass. A weak supercontinuum signal was measured when only a 530-nm laser pulse or a 1060-nm laser pulse was incident into the sample. An enhanced supercontinuum signal was obtained when both 530- and 1060-nm laser pulses were sent through the sample at the same time. This signal is defined as the IUSP, which could arise from the IPM process and/or stimulated four-photon parametric generation (FPPG). The conventional USP generated by one laser beam<sup>1</sup> is attributed to SPM and FPPG processes.

In this IUSP experiment, the SH 530-nm laser pulse intensity was kept nearly constant with pulse energy of about 80  $\mu\text{J}$ . The primary 1060-nm laser pulse energy was a controlled variable changing from 0 to 2 mJ. Filters were used to adjust the 1060-nm pump-laser intensity. The output beam is separated into three paths for diagnosis.

The output beam along path 1 was imaged onto the slit of a 0.5-m Jarrell-Ash spectrograph to separate the contributions from the possible different mechanisms of the supercontinuum by analyzing the spatial distribution of the spectrum from phase-modulation (PM) and FPPG processes. In this spectrograph measurement, films were used to measure the spatial distribution of the emission supercontinuum spectrum and a photomultiplier tube was used to obtain quantitative readings. To distinguish different contributions from either PM or FPPG, geometrical blocks were arranged in the path for the selection of a particular process. An aperture of 6-mm diameter was placed in front of the entrance slit of the spectrograph to measure the PM contributed signal, while an aluminum plate of 7-mm width was placed in front of the spectrograph entrance slit to measure the FPPG contribution.

The beam along path 2 was directed into a spectrometer with an optical multichannel analyzer to measure the supercontinuum spectral intensity distribution. The spectrum was digitized, displayed, and stored into 500 channels as a function of wavelength. The beam along path 3 was delayed and directed into a

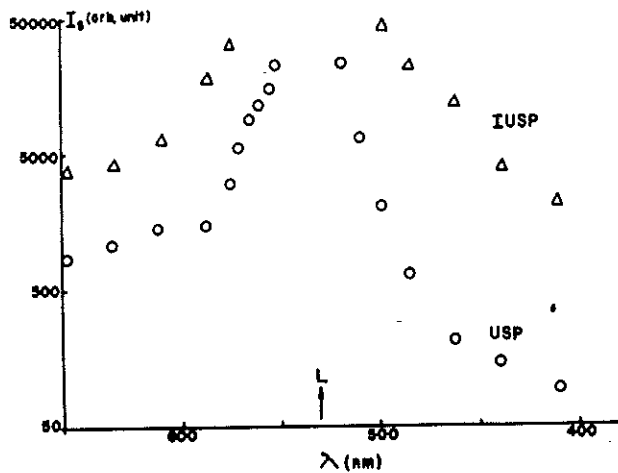


Fig. 1. Intensity of IUSP and USP as a function of wavelength. Each data point was an average of about 20 laser shots and corrected for the detector, filter, and spectrometer spectral sensitivity.  $\Delta$ , IUSP;  $\circ$ , USP from 530 nm. USP from 1060 nm, which is not shown here, was  $\approx 1\%$  of the IUSP signal. The measured 530-nm probe pulse was about  $5 \times 10^8$  counts in this arbitrary unit scale. The error bar of each data point is about  $\pm 20\%$ .

Hamamatsu Model C1587 streak camera<sup>8</sup> to measure the temporal distribution of the laser pulses and IUSP. The duration of IUSP with a selected 10-nm bandwidth was measured to be about the same as the incident laser-pulse duration.

Experimental results of the spectral distribution of IUSP and USP are displayed in Fig. 1. More than 20 laser shots of each data point in each instance have been normalized and smoothed. The average gain of IUSP in a BK-7 glass from 410- to 660-nm wavelength was about 11 times that of USP. In this instance, both the 530- and 1060 nm laser pulse energies were maintained to be nearly constant:  $80 \mu\text{J}$  for 530 nm and 2 mJ for 1060 nm. In this experiment, the 530-nm laser pulse generated a weak USP and the intense 1060-nm laser pulse served as a catalyst to enhance the supercontinuum in the 530-nm pulse. The USP generated by the 1060-nm pulse alone in this spectral region was less than 1% of the total IUSP. The spectral shapes of USP and IUSP in Fig. 1 have a similar spectral distribution. Use of several liquid samples such as water, nitrobenzene,  $\text{CS}_2$ , and  $\text{CCl}_4$  has also been attempted to obtain the IUSL. There was no significant (2 times) enhancement from all other samples that we tested.

A plot of the intensity dependence of IUSP is displayed in Fig. 2 as a function of the 1060-nm pump-pulse energy. The wavelengths plotted in Fig. 2 were  $\lambda = 570$  nm for the Stokes side and  $\lambda = 498$  nm for the anti-Stokes side. The 530-nm pulse energy was set at  $80 \pm 15 \mu\text{J}$ . The IUSP increased linearly as the added 1060-nm laser pulse energy was increased from 0 to  $200 \mu\text{J}$ . When the 1060-nm pump pulse was over 1 mJ, the supercontinuum enhancement reached a plateau and saturated at a gain factor of about 11 times over the USP intensity generated only by the 530-nm pulse. This gain saturation may be due to the trailing edge of the pulse-shape function's being maximally

distorted<sup>9</sup> when the primary pulse intensity reaches a certain critical value. This implies a saturation in the IPM spectral distribution intensity as the pumped primary pulse energy is above 1 mJ, as shown in Fig. 1.

Since the supercontinuum generation can be due to either the PM and/or FPPG processes,<sup>1</sup> it is important to distinguish between these two different contributions to the IUSP signal. Spatial filtering of the signal was used to separate the two main contributions. The IUSP spectrum shows a similar spatial spectral distribution to that of the conventional supercontinuum.<sup>1</sup> The collinear profile that is due to the PM has nearly the same spatial distribution as the incident laser pulse. Two emission wings at noncollinear angles correspond to the FPPG supercontinuum's arising from the phase-matching condition of the generated wavelengths emitted at different angles from the incident laser-beam direction.<sup>1</sup> Using a photomultiplier system and spatial filtering, quantitative measurements of IUSP contributions from the collinear IPM and that noncollinear FPPG parts were obtained (Fig. 3). These signals, measured at  $\lambda = 570$  nm from the collinear and noncollinear parts of the IUSP, are plotted as a function of the pump-pulse energy. There was little gain from the contribution of FPPG process over the entire added pulse-energy-dependent measurement, as shown in Fig. 3. The main enhancement process of the IUSP generation is consequently attributed to the induced-phase modulation mechanism, which corresponds to the collinear geometry. Another possible mechanism of the observed IUSP could be associated with the enhanced self-focusing of the SH pulse induced by the primary pulse. There was no significant difference in the spatial-intensity distribution of the 530-nm probe beam with and without the added intense 1060-nm pulse.

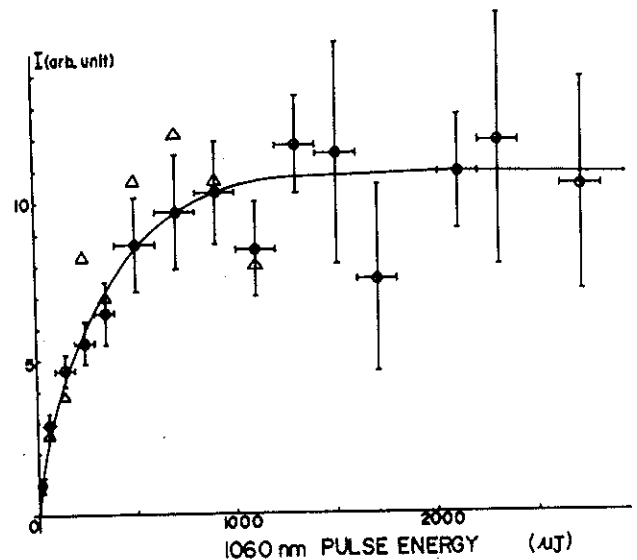


Fig. 2. The dependence of the IUSP signal as a function of the intensity of the 1.06-nm pump pulse.  $\circ$ , the Stokes side at  $\lambda = 570$  nm;  $\Delta$ , the anti-Stokes side at  $\lambda = 498$  nm. The error bar for  $\lambda = 498$  nm measured was similar to that of the Stokes side. The solid line is for an eye guide. The vertical axis is the normalized  $I_{\text{IUSP}}/I_{530 \text{ nm}}$ .

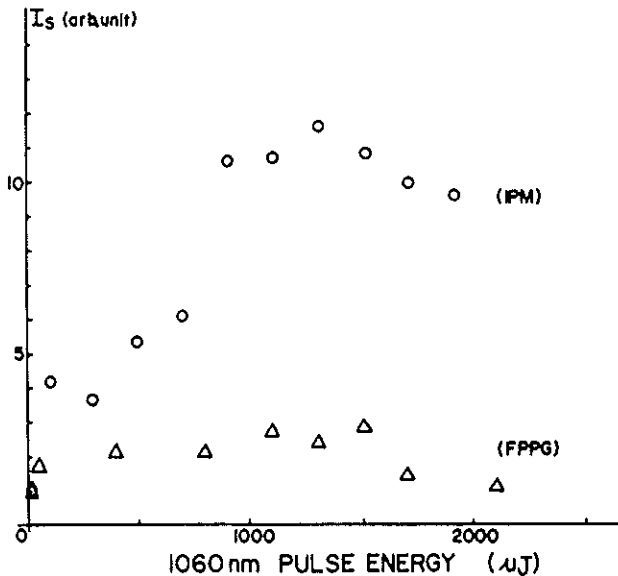


Fig. 3. The dependence of  $I_s$  (IPM) and  $I_s$  (FPPG) at  $\lambda = 570$  nm as a function of the intensity of the 1060-nm pump laser pulse.  $\circ$ , IPM;  $\Delta$ , FPPG. The measured signal has been normalized with the incident 530-nm pulse energy. The error bar of each data point is about  $\pm 20\%$  of the averaged value.

From our previous theoretical analysis of USP<sup>9</sup> and IUSP,<sup>7</sup> the solution of the electric field of the nonlinear wave equation in this system can be expressed as

$$E = E_0 \{ a \exp(i\alpha) \exp[i(kz - \omega t)] + \delta b \exp(i\beta) \times \exp[2i(kz - \omega t)] \}, \quad (1)$$

where  $E_0$  is the electric amplitude of the primary incident pulse,  $\delta$  is the relative strength of the SH signal to the primary frequency signal,  $a$  and  $b$  are the pulse-shape functions of the primary and the SH signals, and  $\alpha$  and  $\beta$  are the phases of these two pulses, respectively. For  $\delta \ll 1$ ,  $b$ ,  $\alpha$ , and  $\beta$  can be derived from the given value of  $a$ .

Neglecting the fast-oscillating terms in  $\chi^3$  and assuming that the group velocity is constant, quasi-linear partial differential equations for  $a$ ,  $b$ ,  $\alpha$ , and  $\beta$  can be deduced. The equations for  $a$  and  $\alpha$  are identical to Eqs. (28a) and (29a) of Ref. 7, while those for  $b$  and  $\beta$  differ from Eqs. (30a) and (31a) through the replacement of  $\epsilon$  by  $\epsilon/2$ . If the primary and SH pulses have the same duration, then the solutions are  $\beta = 2\alpha$  and  $a = b$ , with expressions of  $a$  and  $\alpha$  the same as given in Ref. 9. If the primary and SH lasers have the same duration,  $\beta = 2\alpha$  and  $a = b$ , where expressions of  $a$  and  $\alpha$  are the same as those given in Ref. 9. Consequently, the ratio of the magnitude  $a/b$  is constant throughout the BK-7, i.e., the ratio of the energy densities in the primary ( $a$ ) and SH ( $b$ ) pulses is preserved. Thus the primary pulse modulates the SH pulse only through the index-of-refraction change. There is no direct energy transfer from the primary to the IUSP. The total energy of the radiation centered at  $\omega_2$  at any given location of the glass should be a constant value.

In the measurement, it is difficult to determine how much energy was gained or lost because less than 1% of the SH pulse energy has transferred to IUSP. This constancy of  $a/b$  ratio may be checked using a femto-second pulse where larger conversion efficiency is present. Furthermore, using the scaling of the spectral distribution at different induced-refractive-index change, the IUSP follows the source scaling laws. This means that the IUSP spectral distribution of the SH pulse should have the same spectral distribution as that of the USP of the primary pulse. This is difficult and will be investigated in the future to measure the infrared USP distribution around the 1060-nm wavelength. However, for small  $n_2 E_0^2 z / (c\tau)$ , the USP generated by 530 nm is almost geometrically similar to the spectral distribution of the USP generated by 1060 nm. That means that the spectral distributions of USP and IUSP are almost geometrically similar, as shown in Fig. 1.

The probe-pulse energy should be as small as possible (i.e.,  $\delta \ll 1$ ) for a meaningful comparison of IPM theory and experiment. There should not be any SPM generated from the weak SH pulse shown in Fig. 1. The spectrally broadened signal generated from IPM around  $\omega_2$  experimentally competes with the SPM generated by  $\omega_1$ , which extends from the  $\omega_1$  (1060-nm) to the  $\omega_2$  (530-nm) region and beyond. If  $E(\omega_2)$  is negligible, the intensity of the spectral broadening around 530 nm generated by IPM will be less than the SPM generated by the intense pump pulse. The best combination of the intensity ratio of 1060- and 530-nm pulses has been determined as we described before. The enhancement of the spectrally broadened signal around 530 nm was  $>10$  times when the pulse energy of the weak probe laser was set to be 80  $\mu\text{J}$ . This is a clear evidence of IPM.

This research is supported by Hamamatsu Photonics KK, the National Science Foundation Office of Interdiscipline Research, and the U.S. Air Force Office of Scientific Research.

## References

1. R. R. Alfano and S. L. Shapiro, *Phys. Rev. Lett.* **24**, 584, 592, 1217 (1970).
2. R. R. Alfano, ed., *Biological Events Probed by Ultrafast Laser Spectroscopy* (Academic, New York, 1982); *Semiconductors Probed by Ultrafast Laser Spectroscopy* (Academic, New York, 1984), Vols. 1 and 2.
3. S. L. Shapiro, ed., *Ultrashort Light Pulses* (Springer, New York, 1977); R. A. Fisher, ed., *Optical Phase Conjugation* (Academic, New York, 1983).
4. R. L. Fork, C. V. Shank, C. Hirlimann, and R. Yen, *Opt. Lett.* **8**, 1 (1983).
5. J. T. Manassah, P. P. Ho, A. Katz, and R. R. Alfano, *Photonics Spectra* (November 1984), p. 53.
6. R. H. Stolen and C. Lin, *Phys. Rev. A* **17**, 1448 (1978).
7. J. T. Manassah, M. A. Mustafa, R. R. Alfano, and P. P. Ho, *Phys. Lett.* **113A**, 242 (1985).
8. Q. X. Li, T. Jimbo, P. P. Ho, and R. R. Alfano, *Appl. Opt.* **12**, 1869 (1986).
9. J. T. Manassah, M. Mustafa, R. Alfano, and P. P. Ho, *IEEE J. Quantum Electron.* **QE-22**, 197 (1986).

